Scanning Synchrotron X-Ray Fluorescence Microanalysis for Tephrochronological Studies

A. V. Darin[a], *, F. A. Darin[b, c], **, D. S. Sorokoletov[b], Ya. V. Rakshun[b], and D. Yu. Rogozin[d]

[a] Sobolev Institute of Geology and Mineralogy, Siberian Branch, Russian Academy of Sciences, Novosibirsk, 630090 Russia
[b] Budker Institute of Nuclear Physics, Siberian Branch, Russian Academy of Sciences, Novosibirsk, 630090 Russia
[c] Center for Collective Use "Siberian Circular Photon Source" (SKIF), Boreskov Institute of Catalysis, Siberian Branch,
Russian Academy of Sciences, Novosibirsk, 630559 Russia
[d] Institute of Biophysics, Siberian Branch, Russian Academy of Sciences, Krasnoyarsk, 660036 Russia
*e-mail: Darin@ngs.ru
**e-mail: F.A.Darin@inp.nsk.su

Abstract—On the border of China and North Korea, there is the only active stratovolcano in the eastern part of Asia: Mount Paektu (other names are Baitoushan and Changbaishan). It is widely known for one of the largest eruptions in the historical era, which occurred in the 10th century AD. On the volcanic-activity scale, the event is rated at seven points, this is the largest eruption in the last millennium. Modern research shows that the eruption of the Paektu volcano occurred in late autumn–winter 946 AD. This dating is supported by data obtained from the study of an ice core from North Greenland, in which traces of volcanic ash were found. At a depth of 860 mm (the age according to the calculation of annual layers is 942 AD ± 26 years), a layer 2–3 mm thick was found, which differed sharply in color and texture from the rest of the core material. Using a module of confocal X-ray microscopy, an optical section containing an anomalous layer was studied. 2D scanning with a focused beam of synchrotron radiation 20 μm in diameter was carried out. A large amount of microparticles with a high content of zirconium and yttrium was found inside the layer. The possibility of finding traces of the eruption of the Paektu volcano is discussed.

Keywords: synchrotron radiation, X-ray fluorescence analysis, tephrochronology

DOI: 10.1134/S1027451023060095

INTRODUCTION

The tephrochronology method is based on the fact that each volcanic event produces ash with a unique chemical composition (fingerprint). Explosive volcanic eruptions emit huge volumes of fine ash that can be transported over long distances. Thus, a dated tephra horizon will act as a time stamp in any area. Tephrochronology assumes the unambiguous identification of tephra, which sometimes extends to distances far from the eruption site [1].

Examples of identification of tephra layers at distances of several thousand kilometers are known. In southwestern Russia, an ash layer of distal fine-grained tephra with a grain size of 60–170 μm is widespread and is dominated by highly elongated fragments of glass. Chemical analysis confirms that this layer correlates with the known Y5 ash layer in marine cores in the southeastern Mediterranean. It is shown that the ash particles were scattered over distances of more than 2500 km from the source located in Italy [2]. The chemical composition of microparticles confirmed the ash of the Kamchatka volcano Ksudach

KS2 found on Svalbard at a distance of about 5000 km from the volcano [3]. Microscopic layers of cryptotephra in sediments from around the world indicate that explosive volcanic eruptions have caused ash to fall in many regions, several thousand kilometers from active volcanoes.

To establish a reliable correlation between tephra layers found in different places, its geochemical characterization (fingerprint) is necessary. Traditionally, tephra layers are determined geochemically and petrographically by analytical methods with a high spatial resolution: electron-probe microanalysis or inductively coupled plasma mass spectrometry with laser ablation [4]. However, this process is destructive and laborious, which complicates the use of tephra as isochrones of known age, especially in bottom-sediment cores.

X-ray fluorescence microscopic analysis (micro-XRF) of bottom-sediment cores is a fast, nondestructive method that requires minimal sample preparation [5]. The possibility of quickly and reliably identifying tephra using micro-XRF core scanners looks promis-

Table 1. Eruptions of the last millennium with the index VEI-7

Volcano/region/hemisphere	Date, AD	Emissions, km^3	Column height, km
Tambora/Indonesia/Southern	1815	160–213	43
Kuwae/Vanuatu/Southern	1452–1453	60–108	–
Samalas/Indonesia/Southern	1257	130–200	–
Paektu, Baitoushan, Tianchi/Korea/Northern	944–947	120	25–36

ing. The potential of the use of micro-XRF scanners is also associated with the ability to locate cryptotephra, which are invisible to the naked eye [6]. The use of synchrotron radiation (SR) instead of an X-ray tube for scanning micro-XRF significantly improves the analytical capabilities of the method by reducing the limits of detection and expanding the set of detectable elements [7].

SR is characterized by a continuous spectrum, low divergence, high photon flux, and linear polarization, making it an ideal source for high-precision XRF. The modern version offers elemental visualization with a high spatial resolution (from 0.5 to 10 μm), which makes it possible to solve many problems in life sciences, Earth and environmental sciences, in medical applications, and archaeological and cultural-heritage studies [8, 9].

Therefore, scanning micro-XRF [10] is used as a tool for the in situ search for aerosol microparticles in bottom sediments.
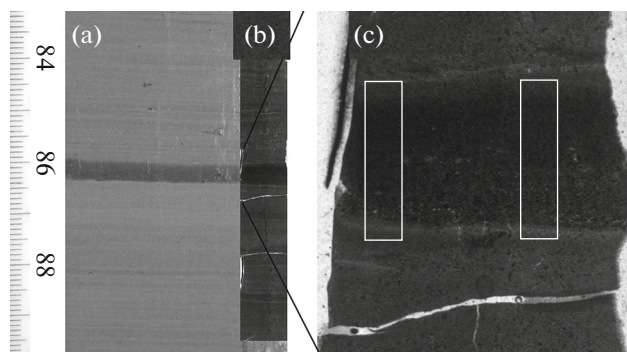
OBJECT OF STUDY

To measure the power of volcanic eruptions, the VEI index (Volcanic Explosivity Index) is most commonly used. This is a comprehensive assessment of the explosive nature of an eruption [11], which is related to the volume of tephra ejected from the magma cham-

ber into the atmosphere. The range of the VEI index is from zero (emissions less than 10^4 m^3) up to eight (emissions 10^{12} m^3 and the height of the ash column is more than 25 km). The scale is logarithmic from VEI-2 and above, i.e., an increase in the index by one indicates an eruption 10 times more powerful. At least four (Table 1) of the most powerful eruptions with the index VEI-7 are known to have occurred in the last millennium [12–14].

The 10th century Paektu volcanic eruption is the only one of the largest in the world in the last millennium that occurred in the northern hemisphere. Explosive material (so-called Baekdusan-Tomakomai, or B–Tm, tephra is a key layer of the eruption of the Paektu volcano) was scattered over a vast territory, up to Greenland (about 7000 km from the volcano) [15]. Given the volume and global nature of the impact of emissions from this volcano, there is a high probability of finding traces of it in various places on the planet. The choice of deposited material and the analytical tool used are important.
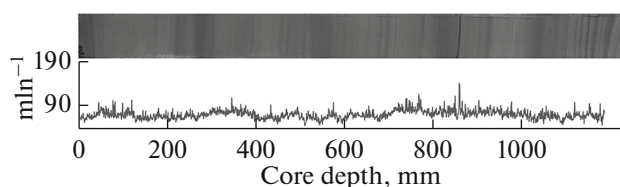
In the present study, the deposited material is the bottom sediment of Lake Bele (Khakassia), which contains annual layers (varves). In the Bele-2012 and Bele-2014 cores obtained in different parts of the lake, a dark layer 3–4 mm thick is visually distinguished (Fig. 1a). Varve-chronology dating of the dark layer gives an age estimate of 942 ± 26 AD, which coincides within the error with modern estimates of the date of the Paektu eruption. To carry out the research, an optical section 20 μm thick from the Bele-2014 core interval was used, containing the dark layer (Figs. 1b and 1c).

EXPERIMENTAL

The search and study of microparticles was carried out according to the scheme previously used to study palladium particles in chromite ores of the Bushveld complex [16]. At the initial stage, the one-dimensional scanning of core samples made from solid preparations of bottom sediments impregnated with epoxy resin was carried out according to the procedure in [17]. The scanning parameters were: excitation energy of 21 keV, collimated SR beam 0.5 mm in core height and 2 mm in width, and a scanning step of 0.6 mm. The results of one-dimensional scanning revealed a geochemical anomaly in the region of the dark layer, char-

Fig. 1. Bottom sediment of Lake Bele (Khakassia): (a) initial (wet) core of Bele-2014, a dark layer is visible in the range of 860–864 mm, different in color and thickness from the rest of the core intervals; (b) optical section B-50, covering the core interval of 830–895 mm; (c) a fragment of section B-50; rectangles mark the areas scanned by micro-XRF with SR excitation.

Fig. 2. Distribution of the zirconium content over the depth of the Bele-2014 core according to one-dimensional scanning data with a step of 0.6 mm by micro-XRF with SR excitation. In the interval of 860−865 mm, a geochemical anomaly is identified, which coincides with the marker bed(dark stripe in the core photo).

acterized by elevated concentrations of zirconium and yttrium (Fig. 2).

To search for and identify individual microparticles inside the layer under study, which differ in elemental composition from the enclosing matrix, we used the Confocal X-ray microscope developed at the Budker Institute of Nuclear Physics, Siberian Branch, Russian Academy of Sciences [18, 19]. To refine the characteristics of the geochemical anomaly, two-dimensional scanning of the optical section was performed (B50, depth interval of 830−895 mm of the Bele-2014 core). We studied two regions with dimensions of 6.0 × 1.0 mm, crossing the marker bed (Fig. 1c). The experimental parameters were: excitation energy of 21 keV, scanning step within a row of 50 and 100 μm, and a distance between rows of 200 μm. The mode of partial defocusing of the excitation-radiation spot on the sample with a size of 50 μm was used in the experiment. Some of the results are shown in Fig. 3.

To refine the morphology and composition of individual particles detected in the defocused mode, we performed a detailed scan of two regions inside the anomalous layer with dimensions of 320 × 420 and 100 × 100 μm. The spot of excitation radiation with an energy of 19 keV was focused to 15 μm. The scanning step in both directions was 20 μm. Two particles are outlined, which stand out sharply in terms of the content of yttrium, zirconium, and a number of other elements. Microparticles differ from each other both in terms of the absolute content of yttrium and zirconium and in the localization of these elements. The first particle is predominantly zirconium with delocalized yttrium (Fig. 4a). The second one has a local (20 × 20 μm) high yttrium content and a blurred distribution of zirconium (Fig. 4b).

DISCUSSION

An optical study of the dark layer showed a structure characteristic of the formation of an annual layer, i.e., the presence of large-sized particles in the lower part (bottom) and small-sized particles in the top of the layer. The mechanism of the formation of such layers is associated with the influx of terrigenous material from the catchment area during spring floods and summer rains, the rapid settling of large-sized, denser particles in autumn, and completion of the annual sedimentation cycle in winter with the formation of the top of the layer containing fine-sized particles. It can be argued that the formation of the dark layer is associated with a short-term event that significantly changed the external conditions of the region. The amount and composition of the incoming material dif-
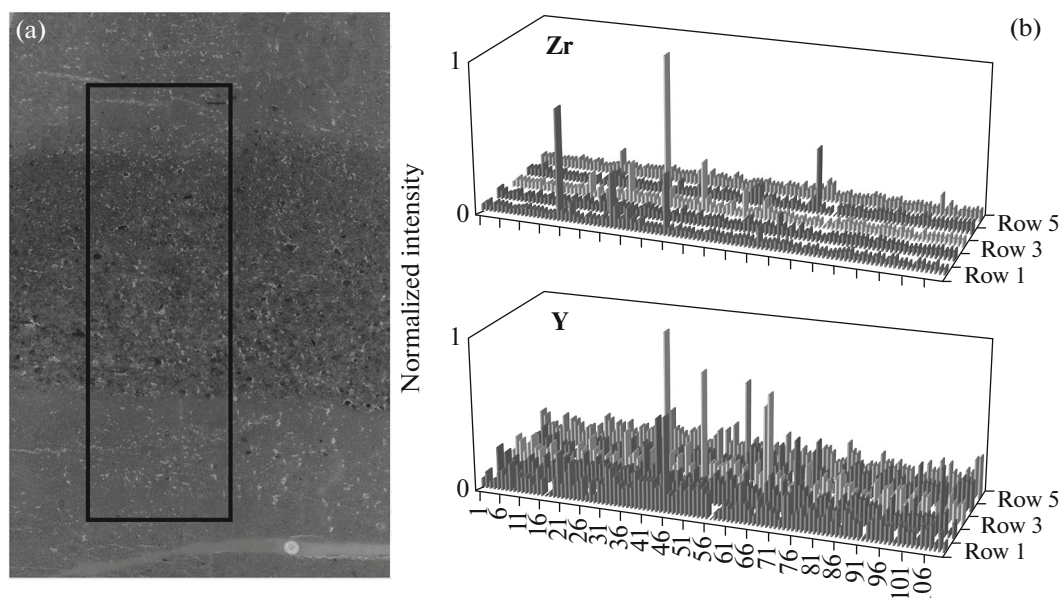
Fig. 3. Fragment of the thin section B-50 with selected scanning area (a) and 2D distributions of Zr and Y (5 rows of 120 points) (b).

(a)

Zr Y

(b)

Zr Y
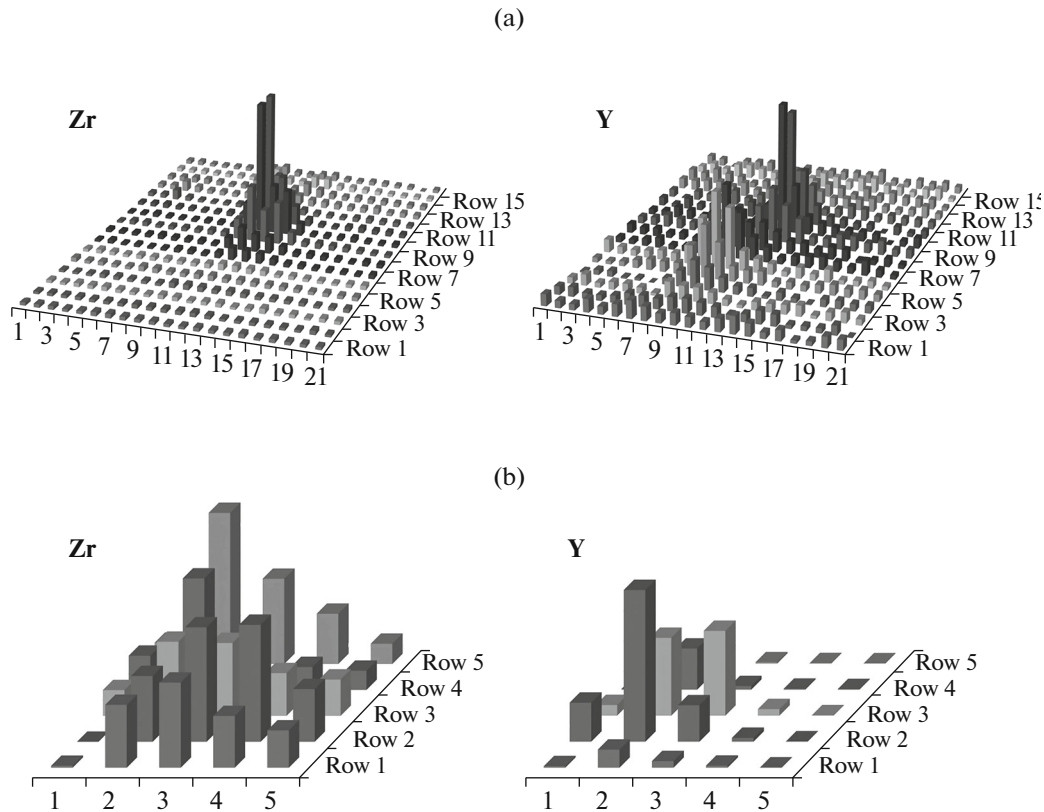
Fig. 4. 2D distribution of two contoured microparticles (spot of excitation radiation 15 μm, step 20 μm in both directions): (a) rounded zirconium–yttrium particle 20–30 μm in size μm (the greatest content of yttrium coincides with that of zirconium; another local yttrium particle with the size 40 × 20 μm is observed); (b) zirconium particle 60 × 40 μm in size, interspersed with an yttrium particle 20–30 μm in diameter.

fers from the adjacent core intervals, which also indicates the event-driven nature of dark-layer formation.

The studied layer differs from neighboring core intervals not only in terms of the presence of yttrium–zirconium microparticles, but also in terms of the overall Br/Rb ratio (Fig. 3b). In bottom sediments, the content of bromine, as a rule, correlates with the input of organic matter of both allochthonous and autochthonous origin. A noticeable decrease in the Br/Rb ratio can be interpreted as a single input of a large amount of material depleted in organic matter. The source of such material can be an aerosol, e.g., volcanic ash. The sizes of the investigated yttrium–zirconium microparticles are in the range of 20–60 μm. This is quite comparable with the grain sizes of 60–170 μm noted in publications, found at a distance of more than 2500 km from the source [2].

Since the main studies of B–Tm tephra were carried out with isolated particles of volcanic glass and mainly oxides of rock-forming elements were determined [20, 21], the in situ data on the composition of microparticles obtained in this work do not allow an unambiguous comparison with the ash of Mount Paektu. But we can confidently state that the studied anomalous layer in the bottom sediments of Lake Bele

is associated with an event that occurred in the interval 916–968 AD, which is characterized by the appearance of a large amount of aerosol substance of a specific elemental composition.

CONCLUSIONS

The used micro-XRF method with SR excitation makes it possible to detect in situ and isolate individual microparticles in the matrix of lacustrine bottom sediments by differences in elemental composition. Microparticles found in the core of the bottom sediments of Lake Bele, judging by the dating and composition, may be traces of the largest eruption of the Paektu volcano in the 10th century. For further studies, it is required to isolate microparticles from the sediment matrix to obtain extended data on the chemical composition for comparison with B–Tm tephra.

The use of micro-XRF with SR excitation for studying bottom sediments in the scanning mode makes it possible to detect layers that differ in elemental composition from the main material of the core and evaluate them for the presence of cryptotephra. The detection and analysis of individual microparticles can provide information on the nature of chemical anom-

alies and determine the need for further research. It can be used not only for solving problems of tephrochronology, but also for the geochemical search for hidden ore occurrences and environmental studies.

FUNDING

CONFLICT OF INTEREST

The authors declare that they have no conflicts of interest.

REFERENCES

1. D. J. Lowe, Quat. Geochronol. **6**, 107 (2011).
   https://doi.org/10.1016/j.quageo.2010.08.003
2. D. M. Pyle, G. D. Ricketts, V. Margari, T. H. van Andel, A. A. Sinitsyn, N. D. Praslov, and S. Lisitsyn, Quat. Sci. Rev. **25**, 2713 (2006).
   https://doi.org/10.1016/j.quascirev.2006.06.0
3. W. G. M. Van der Bilt, C. S. Lane, and J. Bakke, Quat. Sci. Rev. **164**, 230 (2017).
   https://doi.org/10.1016/j.quascirev.2017.04.0
4. C. S. Lane, D. J. Lowe, S. P. E. Blockley, T. Suzuki, and V. C. Smith, Quat. Geochronol. **40**, 1 (2017).
   https://doi.org/10.1016/j.quageo.2017.04.003
5. I. W. Croudace, L. Löwemark, R. Tjallingii, and B. Zolitschka, Quat. Int., **514**, 5 (2019).
   https://doi.org/10.1016/j.quaint.2019.04.002
6. M. E. Kylander, E. M. Lind, S. Wastegard, and L. Lowemark, Holocene **22**, 371 (2011).
   https://doi.org/10.1177/0959683611423688
7. V. B. Baryshev, Yu. P. Kolmogorov, G. N. Kulipanov, and A. N. Skrinskii, Zh. Anal. Khim. **41**, 389 (1986).
8. H. A. Castillo-Michel, C. Larue, A. E. Pradas Del Real, M. Cotte, and G. Sarret, Plant Physiol. Biochem. **110**, 13 (2017).
   https://doi.org/10.1016/j.plaphy.2016.07.018
9. K. Tsuji, K. Nakano, Y. Takahashi, K. Hayashi, and C.-U. Ro, X-Ray Spectrum. **84**, 636 (2011).
   https://doi.org/10.1021/ac202871b
10. A. V. Dar'in, F. A. Dar'in, Ya. V. Rakshun, D. S. Sorokoletov, A. A. Gogin, and R. A. Senin, Geodin. Tektonofiz. **13**, 1 (2022).
    https://doi.org/10.5800/GT-2022-13-2-0581
11. C. G. Newhall and S. Self, J. Geophys. Res.: Oceans **87**, 1231 (1982).
    https://doi.org/10.1029/jc087ic02p01231
12. C. Oppenheimer, Prog. Phys. Geogr. **27**, 230 (2003).
    https://doi.org/10.1191/0309133303pp379r
13. C. Oppenheimer, L. Wacker, J. Xu, et al., Quat. Sci. Rev. **158**, 164 (2017).
    https://doi.org/10.1016/j.quascirev.2016.12.024
14. J. B. Witter and S. Self, Bull. Volcanol. **69**, 301 (2006). .
    https://doi.org/10.1007/s00445-006-0075-4
15. X. -Y. Chen, S. P. E. Blockley, P. E. Tarasov, et al., Quat. Geochronol. **33**, 61 (2016).
    https://doi.org/10.1016/j.quageo.2016.02.003
16. F. A. Darin, D. S. Sorokoletov, Ya. V. Rakshun, A. V. Darin, and I. V. Veksler, J. Surf. Invest.: X-ray, Synchrotron Neutron Tech. **12**, 123 (2018).
    https://doi.org/10.1134/S1027451018010263
17. A. V. Dar'in, I. A. Kalugin, and Ya. V. Rakshun, Bull. Russ. Acad. Sci.: Phys. **77**, 188 (2013).
    https://doi.org/10.3103/S1062873813020123
18. F. A. Dar'in, Ya. V. Rakshun, D. S. Sorokoletov, A. V. Darin, and V. M. Kalugin, Yad. Fiz. Inzh. **8**, 86 (2017).
    https://doi.org/10.1134/S2079562917010067
19. F. Darin, D. Sorokoletov, I. Rakshun, V. Kriventsov, and A. Darin, AIP Conf. Proc. **2299**, 070001 (2020).
    https://doi.org/10.1063/5.0030411
20. D. McLean, P. G. Albert, T. Nakagawa, et al., Quat. Sci. Rev. **183**, 36 (2018).
    https://doi.org/10.1016/j.quascirev.2017.12.013
21. D. McLean, P. G. Albert, T. Nakagawa, R. A. Staff, T. Suzuki, and V. C. Smith, Quat. Sci. Rev. **150**, 301 (2016).
    https://doi.org/10.1016/j.quascirev.2016.08.0